Received: 25 October 2019 | Revised: 24 February 2020 | Accepted: 22 March 2020
DOI: 10.1002/we.2509

WILEY

RESEARCH ARTICLE

Numerical study of a concept for major repair and replacement of offshore wind turbine blades

Wilson Guachamin-Acero[1] | Zhiyu Jiang[2] | Lin Li[3]

[1]Departamento de Ingeniería Mecánica, Escuela Politécnica Nacional (EPN), Quito, Ecuador
[2]Department of Engineering Sciences, University of Agder, Grimstad, Norway
[3]Department of Mechanical and Structural Engineering and Materials Science, University of Stavanger, Stavanger, Norway

Correspondence
Zhiyu Jiang, Department of Engineering Sciences, University of Agder, 4878 Grimstad, Norway.
Email: zhiyu.jiang@uia.no

Abstract

Repair and replacement of offshore wind turbine blades are necessary for current and future offshore wind turbines. To date, repair activities are often conducted using huge jack-up crane vessels and by applying a reverse installation procedure. Because of the high costs associated with installation and removal of offshore wind turbine components and the low profit margin of the offshore wind industry, alternative methods for installation and removal are needed. This paper introduces a novel concept for replacement or installation of offshore wind turbine blades. The concept involves a medium-sized jack-up crane vessel and a tower climbing mechanism. This mechanism provides a stable platform for clamping, lowering, and lifting of a blade. A case study of a 5-MW offshore wind turbine is shown, where common engineering practices were applied and numerical simulations of the marine operations were carried out using finite element and multibody simulation tools. Operational limits for wave and wind actions were established to demonstrate the technical feasibility of the proposed concept.

KEYWORDS

blade replacement, numerical simulation, offshore wind turbine, tower climbing mechanism, wind and waves

1 | INTRODUCTION

The operation and maintenance phase plays an important role in the life cycle of an offshore wind turbine (OWT). Maintenance activities should be well-planned to avoid unexpected failures of OWT components and to reduce unnecessary downtime of OWTs. Common maintenance activities include inspection or replacement of electrical components and scheduled maintenance of key mechanical components like gearboxes. These activities are currently done by personnel who periodically access and inspect critical components of OWTs. Access to an OWT can be achieved using a catamaran vessel or more specialized vessels equipped with actively compensated crew transfer systems.[1] Despite maintenance plans and improved designs of OWTs, major OWT components such as blades, gearboxes, and generators still have relatively high failure rates.[2] Recently, wind turbine blades of the Anholt offshore wind farms off Denmark were brought ashore for repair of leading-edge erosion damage less than 5 years after the wind farm was commissioned in 2013.[3] As the longest announced wind turbine blade has a length close to 200 m, challenges arise when major OWT components such as blades need to be removed and replaced, as these components cannot be easily handled offshore.

Major repair and replacement of these OWT components are often conducted using specialized jack-up crane vessels and by following a reverse procedure of installation. For major repair activities, huge and expensive crane vessels need to be mobilized to the offshore sites. Take the Teesside offshore wind farm for example. In a recent effort to replace the gearbox of an OWT, the marine operation was scheduled for 5 to 6 days, and the Wind Server jack-up crane vessel was employed.[4] Even without considering the time for mobilizing and installing the jack-up vessel, the installation of a single 7-MW OWT blade can take between 4 to 8 h.[5] Moreover, installations of OWT blades and gearboxes are challenging during a mating phase, where shafts and bolts are inserted into holes or guides with only a few millimeters installation gaps. The mating phase during installation of other wind turbine components such as transition pieces onto monopile foundations and float-over operations present similar challenges.[6,7]

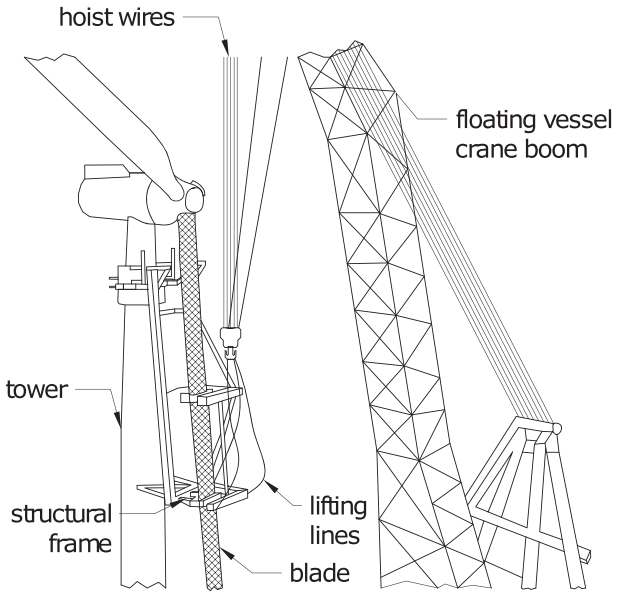

FIGURE 1 A novel blade installation concept using a floating crane vessel, adapted from de Groot [17]

For safe planning and execution of a blade installation using jack-up crane vessels, numerical simulations of related marine operations are necessary. Ren et al.[8] developed a modularized blade installation simulation toolbox for the purpose of control design. Zhao et al.[9] analyzed the installation of an OWT blade considering hydrodynamic and aerodynamic loading on the system and flexibility of structural members. Other recent studies dealt with numerical analysis of OWT blade installation under rough environmental conditions.[10,11] These works investigated the influence of wind parameters on various configurations of the lifting system and set working limits for the wind speed. Moreover, Jiang[12] studied the effect of a tuned mass damping system for monopile foundations in order to reduce the relative motion between the hub and the blade root of an OWT during the installation procedure. In addition to the numerical methods, Maes et al.[13] developed a method for actual motion tracking of a 6-MW OWT blade using a combination of a real-time kinematic global positioning system and the data obtained from an inertial navigation system. The motion tracking is necessary for making decisions on board during critical operations. As shown above, recent developments of new tools and methodologies for better assessment of OWT blade responses during installation using a jack-up crane vessel have been conducted. However, in practice, rental of large crane vessels for such activities is not ideal because of their low availability and high day rate.[5,14] Thus, technically feasible and economically viable alternatives for installation and replacement of major OWT components need to be developed.

Previously, novel procedures for installation of fully assembled OWTs have been proposed by researchers. [6,15,16] However, these procedures are not applicable to installation or decommissioning of a single blade. De Groot[17] proposed an alternative OWT blade installation method; see Figure 1. This method consists of installing an adjustable ring and a structural frame onto the OWT tower using a floating heavy lift vessel. This structural frame includes a stable working platform and a gripper to hold the blade during its positioning and bolting operations. The crane vessel needs to be huge in terms of working height because the frame is clamped to the tower just below the nacelle.

A review of existing literature shows very limited work on developing novel concepts for installation or replacement of blades. Because of the construction of large-scale offshore wind farms in the world, blade replacement is envisaged to be a common activity in future, and thus, this topic needs further research. This paper first introduces a novel procedure for blade replacement. Numerical simulations of potentially critical installation activities are conducted. Finally, the feasibility of the proposed concept is evaluated by assessing the operational limits of the installation activities.

2 | SYSTEM COMPONENTS AND BLADE REPLACEMENT PROCEDURE

The main components of the novel blade replacement concept, the decommissioning procedure, and other practical operational aspects are discussed in this section.

Figure 2A shows main components of the system. These components are the OWT, a medium-sized jack-up crane vessel, and a tower climbing mechanism. The jack-up vessel is required for installing the tower climbing mechanism, transferring of personnel, and lifting or lowering of a blade. Figure 2B shows a schematic of the climbing mechanism. It consists of a lower and and an upper deck, which allocate a gripping system composed of rotating arms, a braking system with friction pads, and two hydraulic cylinders. A hydraulic power pack, winches, and other mechanical drives are located on the upper deck.

2.1 | Tower climbing mechanism

The tower climbing mechanism is inspired by the work developed by Lorber and Pampalov[18] and Sadeghi and Moradi.[19] These concepts have been designed and tested for climbing poles, which are cylindrical structures that resemble wind turbine towers.

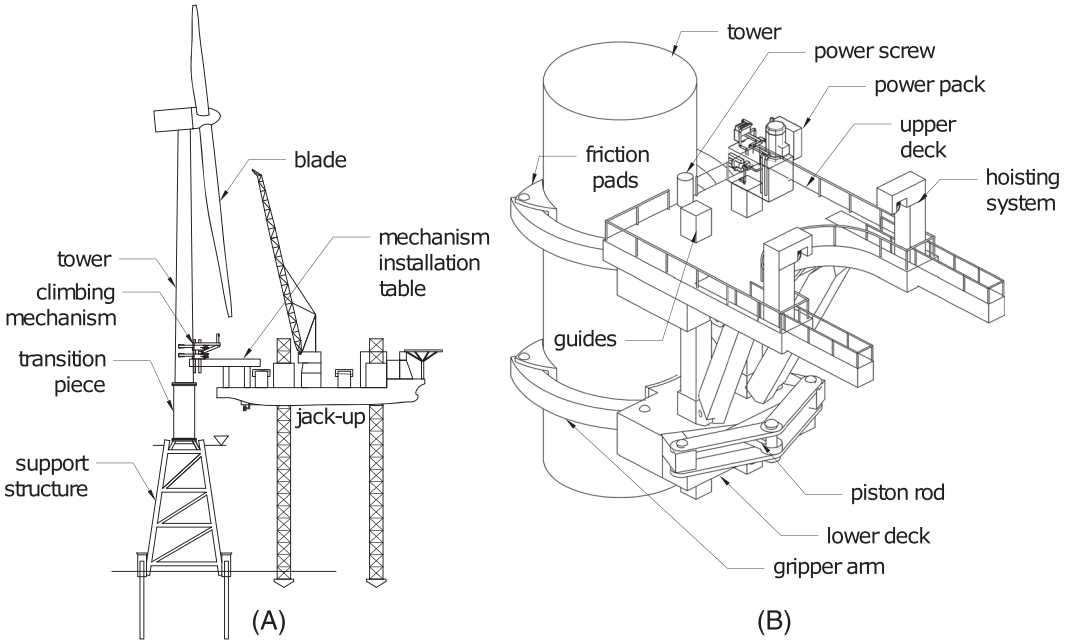

FIGURE 2 A, Main components of a novel blade replacement procedure; B, isometric view of the tower climbing mechanism

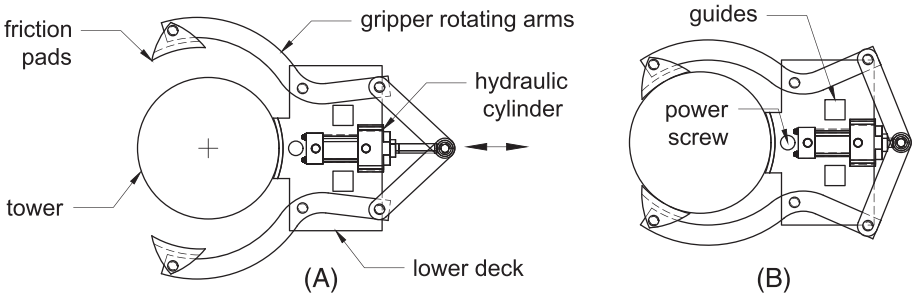

FIGURE 3 Top view of the gripper mechanism. A, Opened position; B, closed position

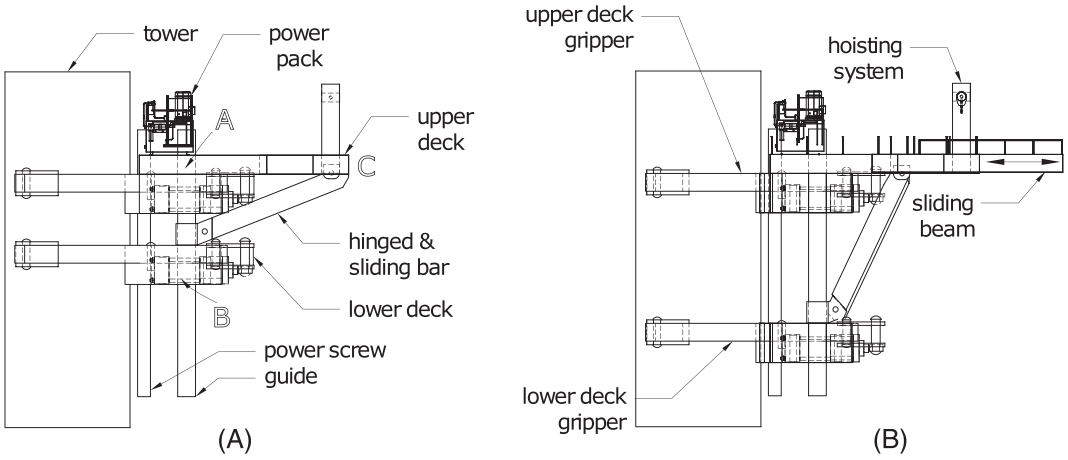

FIGURE 4 Side view of the tower climbing mechanism. A, Retracted condition; B, extended condition

The tower climbing mechanism is intended for climbing the tower, and the mechanism is powered by means of hydraulic and mechanical drives. Figure 3 A,B illustrates the gripper of the lower deck in opened and closed positions, respectively. The rotating arms can be opened or closed by extending or retracting the piston rod of the hydraulic cylinder.

For climbing the tower, the mechanism uses a power screw; see Figure 4A. The drive system for this screw can be either placed on the upper or lower deck. There is also a hinged and sliding bar that adjusts the separation between the lower and upper decks. The hydraulic power pack, hoisting structure, and control systems can be placed on the upper deck. Figure 4A,B shows the mechanism in extended and retracted conditions, respectively.

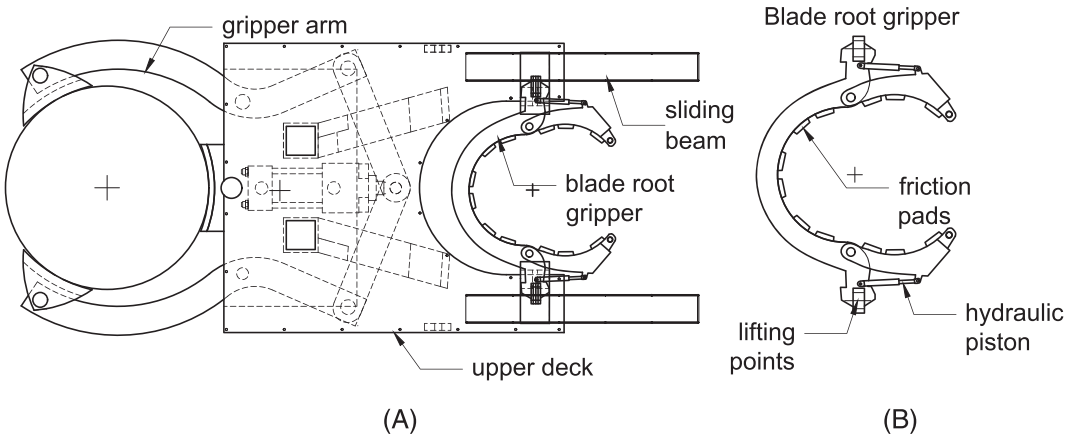

FIGURE 5 Upper deck and blade root gripper. A, Upper deck and blade gripper; B, blade root gripper components

The mode of operation is simple. First, the gripper from the lower deck closes by contracting the piston rod from the hydraulic cylinder. Afterwards, the drive system from the power screw lifts the upper deck, while the hinged and sliding bar rotates and moves. Once the mechanism is in an extended condition, the gripper from the upper deck closes. Then, the gripper from the lower deck opens, and the power screw lifts the deck. Such a process is repeated until the desired elevation of the mechanism is reached. Two guide columns ensure that the mechanism cannot tilt over when only one gripper is secured.

2.2 | Replacement procedure of an OWT blade

The replacement of an OWT blade can be summarized in the following activities:

Positioning of the jack-up crane vessel: A jack-up vessel arrives at the designated offshore site, selects the heading, lowers the legs, and elevates the hull. Figures 2 and 6 illustrate a jack-up vessel already in the operational mode. It can be observed that an installation deck or table can be used to install the tower climbing mechanism on the tower.

Installation of the tower climbing mechanism: The movable installation deck on the vessel can be used to install the tower climbing mechanism; see Figure 2A. After that, the gripper from the lower deck is locked, and the mechanism is ready to climb the tower by following the sequence indicated in Section 2.1.

Tower climbing and blade clamping: The mechanism starts climbing the tower, and at a certain height, it stops and locks itself against the tower; see Figure 6A. This action is necessary for clamping a blade tip gripper that later will be picked up by the crane on board. The mechanism will continue climbing until it reaches a position close to the top of the tower; see Figure 6B, and the mechanism is above the center of gravity (COG) of the blade. At this stage, the hinged and sliding beam from Figure 4A and the gripper arm shown in Figure 5A have to be locked. Once again, a gripper for the blade root (Figure 5B) will be clamped on the blade.

Lowering of the blade: Lifting wires are connected to the lower and upper lifting tools, offshore personnel unbolt the turbine blade from inside the nacelle, and the the blade is lowered onto the deck of the jack-up vessel; see Figure 6C,D.

Change of the blade and departure of the vessel: A reverse procedure can be applied to installation of a new blade. After this procedure is completed, the tower climbing mechanism is lowered and sea-fastened on the deck of the vessel, and the legs of the jack-up crane vessel are lifted up. Finally, the crane vessel can sail away.

A summary of the installation activities and subactivities with the corresponding required installation time is provided in Table 1. The durations of the installation activities are estimated based on industrial experiences of the authors on similar offshore lifting operations. It can be observed that approximately 17 h are required to replace an OWT blade. From this required time, 6 h are spent on the leg lowering and lifting operations of the jack-up vessel, and 11 h are spent on the blade replacement process.

3 | METHODOLOGY FOR FEASIBILITY ASSESSMENT OF THE BLADE REPLACEMENT CONCEPT

This section provides the methodology and necessary information for a numerical feasibility assessment of the proposed blade replacement procedure. This methodology is based on the work of Guachamin Acero,[21] which has been applied to assessment of other types of marine operations.[22,23]

Figure 7 shows that Step 1 corresponds to the development of the blade replacement procedure; see Section 2.2. This procedure is necessary for identifying potentially critical activities (Step 2). The identification can be done using qualitative risk assessment tools like root cause diagrams and meetings with personnel experienced in marine operations. Critical activities are addressed in details in Section 3.1. Step 3 shows that these potentially critical installation activities are selected for numerical modeling; see Section 3.2. A numerical model of each activity is used for

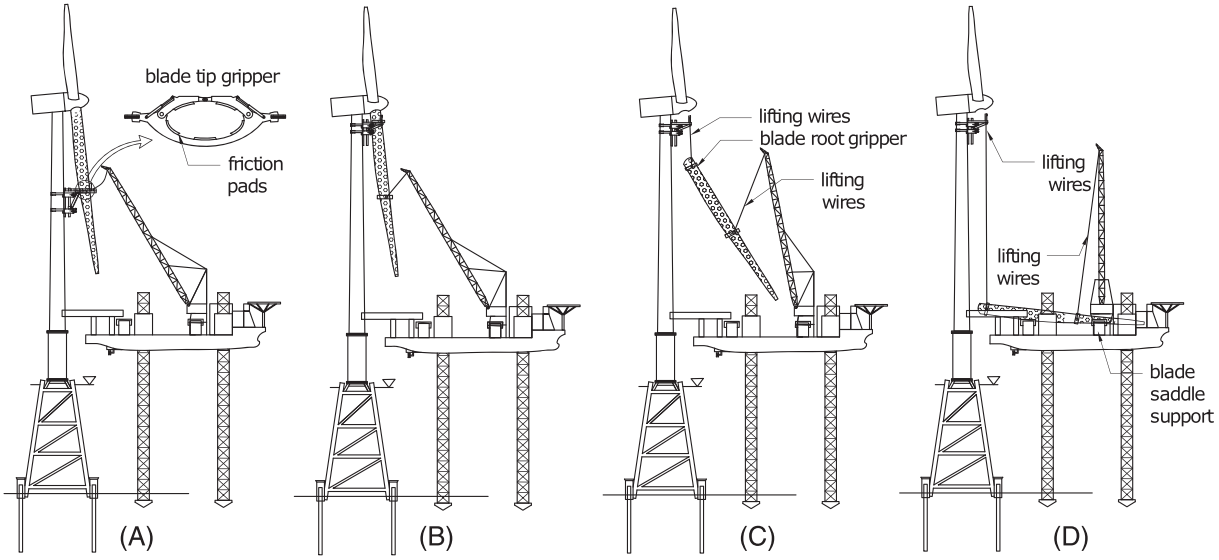

FIGURE 6 Blade replacement. A, Installation of the blade tip gripper using an on-board crane; B, installation of the blade root gripper; C, lowering an offshore wind turbine (OWT) blade; D, blade on deck

TABLE 1 Summary of installation activities and duration

No.	Installation activity	Main subactivities	Duration
1	Positioning/moving jack-up	Leg lowering	3 hours based on a leg lowering speed of
	vessel to location		0.4 m/min and other related operations[20]
2	Installing tower mechanism	Lifting climbing mechanism,	1 h
		connect power supply	
3	Climbing of mechanism	Install blade root and blade	3 h given that the climbing speed
		tip grippers and lifting lines	of 0.05 m/s; see Section 3.2.3
4	Lowering the damaged blade	Unbolt and lower the blade	2 h
		to the deck of the ship	
5	Installing a new blade	Connect lifting lines, lift the	2 h
		blade, bolt the blade	
6	Lower the climbing mechanism	Remove grippers and lifting lines	3 h
7	Moving jack-up vessel from location	Lifting legs	3 h[20]

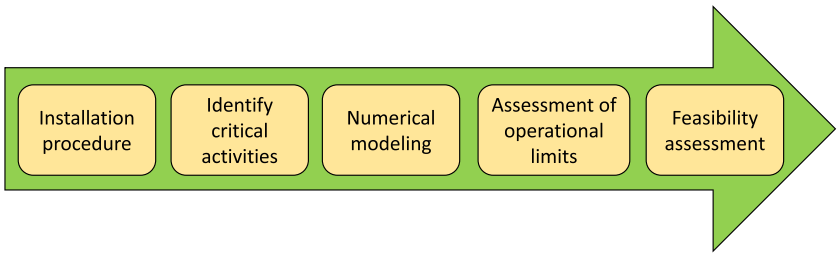

FIGURE 7 Methodology for feasibility assessment of a novel blade replacement procedure [Colour figure can be viewed at wileyonlinelibrary.com]

analysis of critical response parameters, which can be stresses, forces, velocities, displacements, and so forth. Some responses are obtained as results of dynamic action of environmental parameters that could be expressed in terms of environmental parameters including the significant wave height (H_s), wave spectral peak period (T_p) and the mean wind speed (U_w). The relation can be established by comparing the responses with their corresponding allowable limits. The limits of the environmental parameters that cause the responses to reach the same level as the allowable limits are known as operational limits (Step 4), which are derived in Section 4. Based on the operational limits and level of stresses in structural components, an assessment of the feasibility of the proposed concept can be provided (Step 5).

3.1 | Potentially critical installation activities

The proposed blade replacement concept is novel, and thus, some involved operations are not routine activities executed at sea. Nonstandard or new operations that can lead to catastrophic consequences are considered as potentially critical activities.

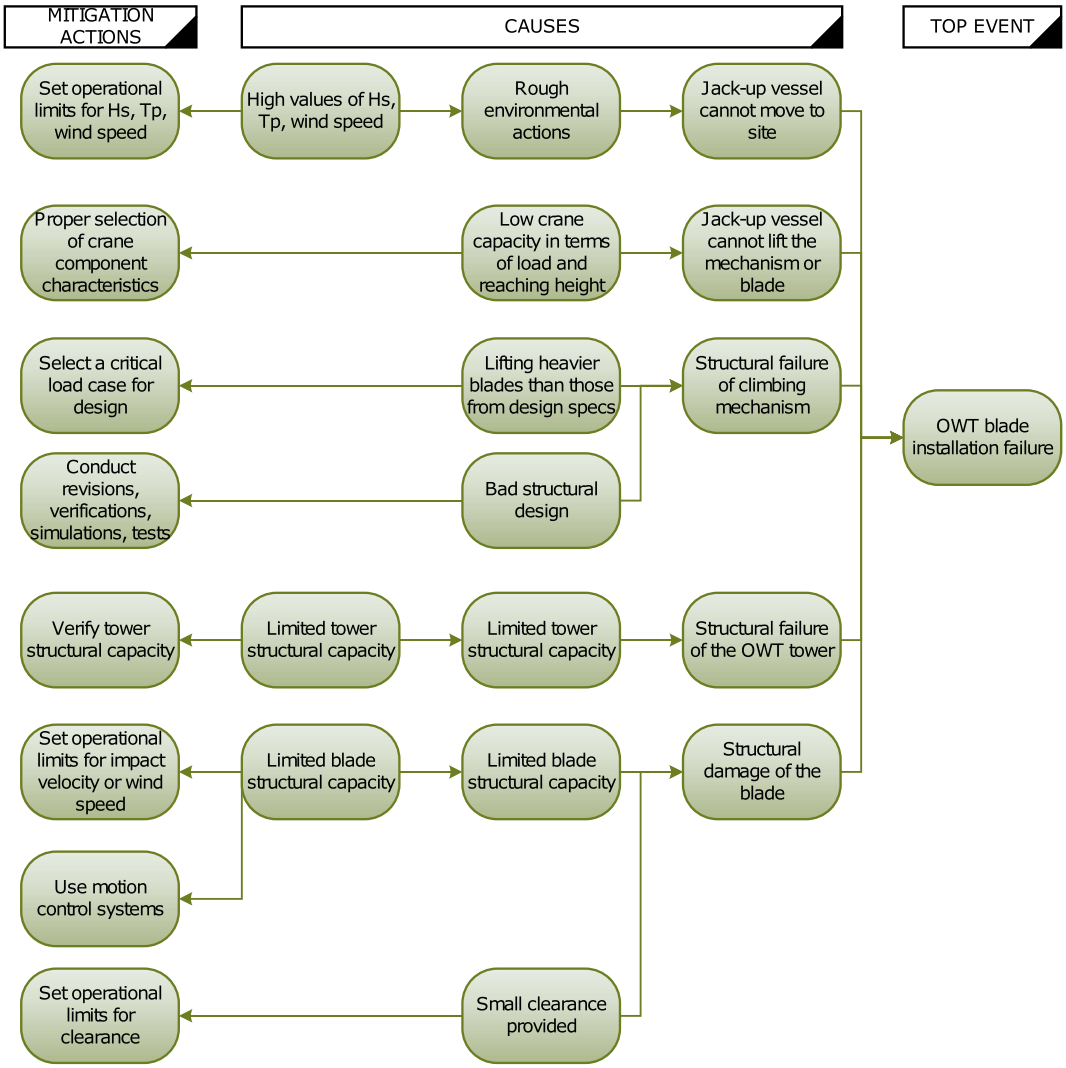

FIGURE 8 Root cause diagram for the novel offshore wind turbine (OWT) blade replacement procedure [Colour figure can be viewed at wileyonlinelibrary.com]

Based on the blade replacement procedure described in Section 2.2, potentially critical installation activities can be identified.[21] Figure 8 presents a root cause diagram, where the OWT blade replacement or installation failure is the main event. This event is a result of other failure events related to installation activities. The cause events occur because response parameters such as stresses and impact velocities can exceed their allowable limits. These responses reach high levels because the environmental parameters including H_s, T_p, and U_w reach unacceptable levels. To reduce the risk of of such failure events, the leftmost column of the diagram gives possible mitigation actions. These actions can help to set limits on the responses or environmental parameters and to avoid failure events.

According to Figure 8, potentially critical activities, corresponding failure events, and response parameters are summarized in Table 2. As mentioned above, these response parameters can be expressed in terms of environmental parameters.

Positioning of the jack-up vessel: Although this is a routine activity, when a jack-up vessel is moving onto a location, a critical scenario occurs when the legs touch the seabed and undergo impact loads. To avoid structural damage, the maximum impact forces that occur must be within allowable limits. These forces depend on impact mass, impact velocity, and mechanical properties of the soil. The impact force is not a practical parameter for onboard decision making, and the environmental parameters or measurable vessel responses are normally desired.[24] A significant wave height of around 1.5 m is a practical value used by the industry,[25] although the origin of such limits is not clear. The H_s limit is not sufficient for floating structures, and T_p and wave direction need be considered.

Climbing of mechanism and clamping to the OWT tower: This activity can be deemed critical, because the tower climbing mechanism can exert large reaction forces on the tower walls. Considering that the tower climbing mechanism is properly designed, one can verify the structural integrity of the tower for a realistic load case that includes the weights of the tower climbing mechanism, equipment on its deck, and the OWT blade. A critical event can be the buckling of the tower due to contact or reaction forces.

Lifting or lowering of the OWT blade: During the blade lifting or lowering operation, the blade can experience large motions because of the action of wind loading and the tugger line system used. In addition, the natural frequencies of the system will continuously change

TABLE 2 Potentially critical activities and limiting parameters

No.	Installation activity	Failure event	Response parameter
1	Positioning/moving jack-up vessel to location	Structural failure of jack-up vessel	Impact velocity between the jack-up leg and the seabed
2	Climbing of mechanism	Structural damage of tower	Stresses or reaction forces on the tower wall
3	Lowering the OWT blade	Structural damage of blade	Impact velocity between the tower and the blade

Abbreviation: OWT, offshore wind turbine.

TABLE 3 Main particulars of the jack-up vessel[28]

Parameter	Symbol	Value	Units
Displacement	∇	6.81×10^4	Ton
Length overall	L_V	60	m
Breadth	B_V	33	m
Draught	T_V	3.6	m
Heave natural period	T_{n_3}	7.1	s
Roll natural period	T_{n_4}	7.5	s
Pitch natural period	T_{n_5}	8.2	s
Leg diameter	Dia_L	1.25	m
Leg length submerged	Len_L	29	m

TABLE 4 Main particulars of structural components of the tower climbing mechanism; refer to Figure 4

Structural member	Description	Maximum service load stress	Weight	Observations
Climbing mechanism				
Frame structure	Square tube W = 0.6 m, H = 0.6 m, t = 0.02 m	σ= 230 MPa	43 kN	W = width, H = height, t = thickness
Gripper structure	Square tube W= 0.8 m, H= 0.8 m, t= 0.05 m	σ= 183 MPa	20 kN	Member DEF Figure 11B
Power screw	D = 0.2 m	stress at thread root σ= 121 MPa	15 kN	D = nominal diameter, pitch = 0.08 m
Other equipment				
Blade, gripper, wire ropes			200 kN	Refer to Table 5
Working deck			100 kN	Assumed
Equipment			100 kN	Assumed

during this process. A critical event can be damage of the composite laminates of a new blade, which can be caused by the impact between the blade root and the tower or between the blade tip and the jack-up crane vessel. Allowable impact velocities can be established based on structural analysis of the impact problem.[26,27]

3.2 | Numerical analysis of marine operations

This section describes the numerical methods for modeling the critical activities listed in Table 2. Responses obtained from numerical analysis of these activities are applied during assessment of operational limits described in Section 4.

3.2.1 | Main particulars of installation system components

In this case study, dynamic analysis of a jack-up vessel under various sea states are performed. The main particulars of the vessel are listed in Table 3. For a detailed description of the jack-up vessel, refer to Jiang et al.[28] The numerical model of the jack-up vessel is described in Section 3.2.2.

Sizing of the main climbing mechanism structural components is prerequisite for assessment of the stresses in the OWT tower. Structural analysis was conducted during the preliminary design of the climbing mechanism. A summary of the main particulars of these structural components is summarized in Table 4 and their details are provided in Section 3.2.3.

The blade-tugger line model includes the NREL 5-MW blade[29] with realistic yoke and tugger line properties. The tugger lines have constant lengths and varying tensions. Table 5 lists key parameters of the system. For the blade structure, the leading edge is parallel to the global *x*-axis; see Figure 9A. The numerical model of the OWT blade lifting system is addressed in Section 3.2.4.

3.2.2 | Positioning of the jack-up vessel

The numerical model of the vessel is established in the SIMO program.[30] The vessel coordinate system and wave directions in the numerical model are defined in Figure 10. The first- and second-order hydrodynamic coefficients of the barge are obtained using the potential flow theory.[31] The second-order loads in surge, sway, and yaw are calculated based on Newman's approximation, and only the difference-frequency part is

TABLE 5 Parameters of the blade and the lifting system

Parameter	Symbol	Value	Units
Blade mass	M_{bd}	17.3	Ton
Blade length	L_{bd}	61.5	m
Blade root diameter	D_{bd}	3.54	m
Distance of blade center of gravity (COG) from root	xb_{COG}	20.57	m
Stiffness of lifting line blade-climbing mechanism	k_w	2×10^5	N/m
Yoke mass	M_{yk}	50	Ton

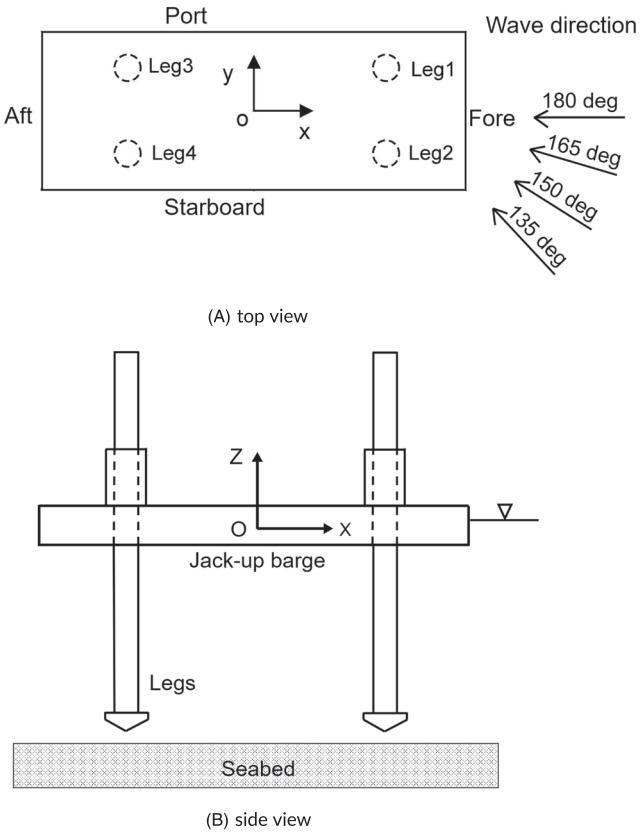

FIGURE 9 Blade configurations for numerical analysis of the decommissioning operation. A, Configuration No. 1 for initial decommissioning phase; B, Configuration No. 2 for final decommissioning phase

considered. Due to the viscous loads on the barge and mooring lines, there exists damping for barge motions. These damping coefficients are represented as linear ones and are selected according to DNV-OS-E301.[32] The barge viscous damping in roll is estimated using the Ikeda formula for barges.[33] The linear damping coefficient is calculated as 1.52×10^8 Nm/(rad/s) at the roll natural period. The viscous effects on the legs are considered by modeling the legs as circular tubes with Morison-type hydrodynamic loading. Because of the capabilities of the SIMO program, no structural mass or entrapped water is considered. Each leg and spudcan is treated as one slender element, which is divided into a number of strips. The horizontal wave force $f_{W,s}$ per unit length on each strip of a vertical moving circular cylinder can be determined using Morison's equation in Equation (1).

$$f_{w,s} = \rho_w C_M \frac{\pi D^2}{4} \cdot \ddot{\zeta}_s - \rho_w (C_M - 1)\frac{\pi D^2}{4} \cdot \ddot{x}_s + \frac{1}{2}\rho_w C_D D \left|\dot{\zeta}_s - \dot{x}_s\right| \cdot (\dot{\zeta}_s - \dot{x}_s). \tag{1}$$

In this equation, the positive force direction is the wave propagation direction. $\ddot{\zeta}_s$ and $\dot{\zeta}_s$ are fluid particle acceleration and velocity at the center of the strip, respectively; $\ddot{x}_s$ and $\ddot{x}_s$ are the acceleration and velocity at the center of the strip due to the body motions; D is the outer diameter of the cylinder. C_M and C_D are the nondimensional mass and quadratic drag force coefficients, respectively, and the values of 2 and 0.9 are applied in the analysis according to DNV-RP-H103.[34]

Time-domain simulations are carried out under various combination of H_s, T_p by solving the equations of motions for the jack-up vessel as shown in Equation (2).

$$(\mathbf{M} + \mathbf{A}(\infty)) \cdot \ddot{\mathbf{x}} + \mathbf{D_1}\dot{\mathbf{x}} + \mathbf{D_2} f(\dot{\mathbf{x}}) + \mathbf{K}\mathbf{x} + \int_0^t \mathbf{h}(t-\tau)\dot{\mathbf{x}}(\tau)d\tau = \mathbf{q}(t, \mathbf{x}, \dot{\mathbf{x}}), \tag{2}$$

where $\mathbf{M}$ is the mass matrix of the jack-up; $\mathbf{x}$ is the rigid-body motion vector with six *DOFs*; $\mathbf{A}(\infty)$ is the added mass matrix for infinite frequency; D_1 and D_2 are the linear and quadratic damping matrices; $\mathbf{K}$ is the hydrostatic stiffness matrix; $\mathbf{h}$ is the retardation function of the vessel,

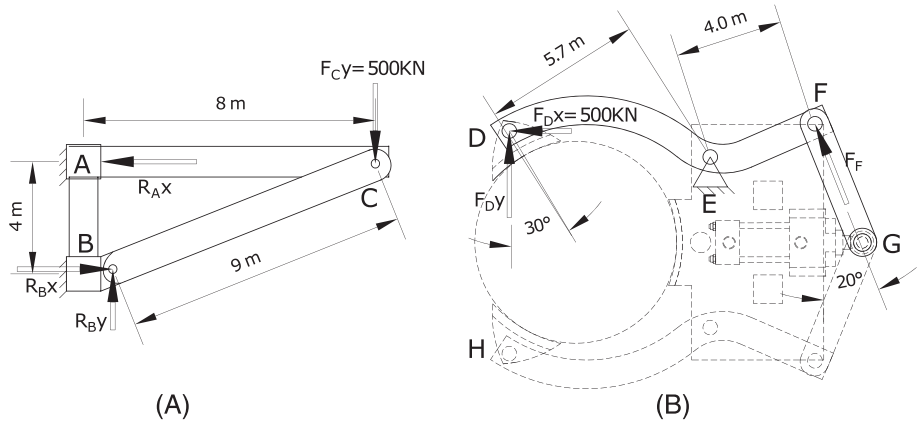

FIGURE 10 Vessel coordinate system and wave directions for numerical analysis of the jack-up vessel under wave conditions

which is calculated from the frequency-dependent added mass or potential damping; **q** is the external force vector that includes the first- and second-order wave excitation forces on the vessel, as well as the wave forces on the legs based on Equation (1).

Four wave directions of 180°, 165°, 150°, and 135° are considered to account for the uncertainties in the wave direction forecast. In practice, operations can also be planned for wave directions different from head seas. Under each condition, six simulations of 500 s are run using different wave seed numbers. In practice, the actual lowering phase during which the jack-up legs touch the seabed normally lasts less than 8 min. Thus, the total simulation length of 3000 s is considered sufficient for assessment of response statistics for a stationary process. Short-crested waves are generated for all sea states using the JONSWAP spectrum and the cosine spreading function.[35]

3.2.3 | Structural assessment of the tower climbing mechanism

As part of the assessment of the novel OWT blade replacement concept, it is necessary to carry out a preliminary design of the mechanism. Moreover, this design is important for the assessment of structural integrity of an OWT tower; see Section 4.2. In the following, a sizing is provided of the structural members and equipment to power the tower climbing mechanism. As shown in Figure 4B, one critical condition is considered of the tower climbing mechanism.

Figure 11A shows a free body diagram for the structure of the tower climbing mechanism. This diagram corresponds to the climbing mechanism configuration shown in Figure 4A. The external load applied at joint C is conservatively estimated as F_C= 500 kN based on the parameters listed in Table 4. It can be inferred that the reaction forces at joint B are as follows: R_Bx= 1000 kN, and R_By= 500 kN. This means that the horizontal reaction force at joint A is R_Ax= 1000 kN, and this force is transmitted to the upper deck gripper friction pads in D and H. For the member DEF shown in Figure 11B, the maximum bending moment in the horizontal plane at point E is M_E= 5700 kNm, and the corresponding force on the locking pin at point F is F_F= 1425 kN.

Based on load-resistance factor design equations recommended by the American Society of Civil Engineers,[36] semiprobabilistic structural design of the climbing mechanism can be conducted using design codes. For the beam DEF, the nominal factored moment strength, $\phi_b M_n$, has to be larger than the factored service load moment, M_u, and the limit-state function can be described by Equation (3) as below:

$$\phi_b M_n \geq M_u, \tag{3}$$

where ϕ_b is the reduction factor for the moment strength. For elastic design, M_n depends on the yield strength F_y and the elastic section modulus Z_x; see Equation (4):

$$M_n = F_y Z_x \tag{4}$$

M_u can be calculated from Equation (5), where M_D is the dead load bending moment and M_L is the live load bending moment, both affected with the corresponding load factors.[36]

$$M_u = 1.2M_D + 1.6M_L. \tag{5}$$

Rotation of member DEF occurs in the horizontal plane, and M_E is due to contributions from M_D=1425 kNm and M_L= 4275 kNm, and thus, Equation (5) gives M_u= 8550 kN. Based on Equation (4), and considering structural steel A572-Gr50, F_y= 345 MPa and Z_x= $3.1\times10^{-2} m^3$, we obtain M_n= 11 000 kNm, which is larger than M_u. Note that tubular sections and ϕ_b= 0.9 are selected[36]; see Table 4. This table also shows the maximum service load stresses in other structural members.

The power required by the screw to move the upper platform in climbing condition (without the weight of the blade) is calculated from Equation (6),[37] where P is the required power, F is the load to raise, d_c is the mean diameter of the collar, d_m is the mean diameter of the screw, f_c is the friction coefficient on the collar, f is the friction coefficient on the threads, v is the climbing velocity, and p is the pitch of the screw. The first term on the right-hand side of the equation corresponds to the torque to overcome the friction in the collar and the thread, and the second

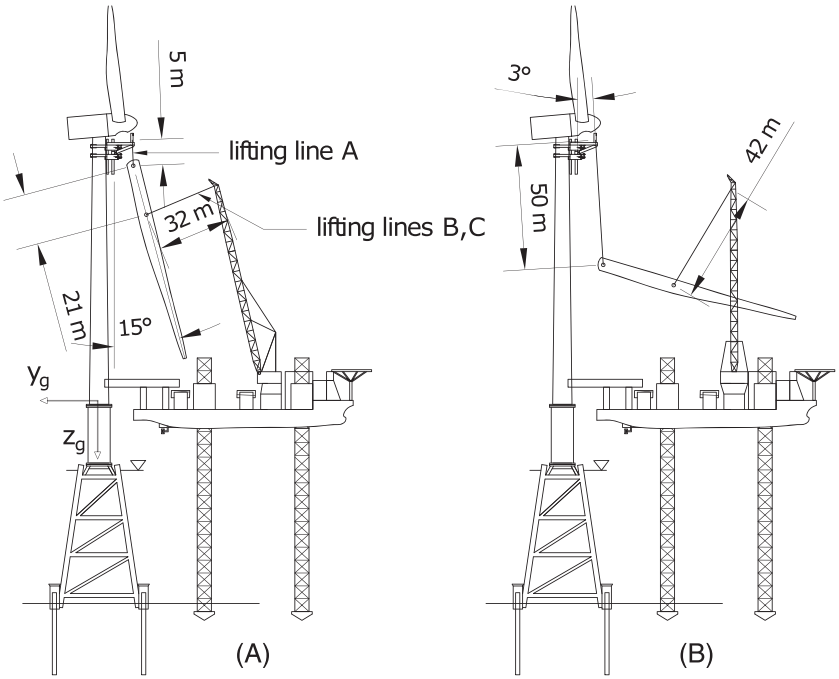

FIGURE 11 Free body diagram. A Frame structure; B, gripper mechanism

term corresponds to the angular velocity of the screw.

$$P = \left(\frac{F f_c d_c}{2} + \frac{F d_m}{2} \frac{(\pi f d_m + l)}{(\pi d_m - f l)} \right) \frac{2\pi v}{p}. \tag{6}$$

Further, considering F= 250 kN, d_c= 0.25 m, d_m= 0.2 m, v= 0.05 m/s, f_c, f= 0.1, and p= 8 mm, the minimum required power to raise the mechanism is approximately P= 250 kW, and the maximum stress at the thread root is 121 MPa.

The fully extended mechanism configuration shown in Figure 4B is critical for the power screw when the mechanism is climbing, and the power screw has a buckling load of 1400 kN, which is much larger than the weight of the tower climbing structure without the weight of the blade, and thus, the designed power screw will satisfy the buckling check. The reaction forces shown in Figure 11A are applied as pressure loads from the friction pads on a section of the OWT tower, for which the stresses are assessed applying the finite element method; see Section 4.2 for a detailed description.

3.2.4 | Numerical modeling of the blade lowering process

The proposed blade lowering procedure is new, and feasibility of the related operations should be demonstrated. As state-of-the-art numerical tools can be used to simulate and represent actual operations, we use numerical simulations to demonstrate the feasibility.

The blade lowering process is nonstationary, and therefore, the dynamic responses should be analyzed by modeling the actual operation.[38,39] In this study, the nonstationary operation is represented by two stationary configurations of the blade lowering lifting system for simplicity. The Configuration No. 1 (Figure 9A) corresponds to the initial phase of the blade lowering operation, whereas the Configuration No. 2 (Figure 9B) represents the final phase. It can be observed that a lifting line (A) is used to connect the tower climbing mechanism to the blade root, whereas two lifting lines (B,C) are used to connect the lifting point on the blade to the crane tip. In the numerical analyses, the lifting points (B,C) on the blade are considered to be close to the COG of the blade, and one end of the lifting lines A, B, or C is rigidly fixed to the ground, ignoring vibrations of the tower climbing mechanism or the crane boom. This simplification applies to jacket support structures subjected to small wave-induced motions.

The horizontal axis wind turbine simulation code 2nd generation (HAWC2), is an aeroelastic code developed by DTU Wind Energy.[40] This code is used to model the blade and lifting lines for the rigging configurations shown in Figure 9. The structural modeling of HAWC2 is based on multibody formulation, in which the floating frame of reference formulation is applied to develop the dynamic formulation of the equations of motion of deformable bodies that have large displacements. [41]

Developed from the Lagrange's equation, the general system differential equations of motion of the multibody system can be written in a matrix form as

$$\mathbf{M}\ddot{\mathbf{q}} + \mathbf{K}\mathbf{q} + \mathbf{C}_q^T \boldsymbol{\lambda} = \mathbf{Q}_e + \mathbf{Q}_v, \tag{7}$$

where $\mathbf{q}$ is the total vector of the system generalized coordinates. $\mathbf{M}$ and $\mathbf{K}$ are, respectively, the system mass and stiffness matrices, C_q is the constraint Jacobian matrix, λ is the vector of Lagrange multipier, Q_e is the vector of generalized externally applied forces, and Q_v is the quadratic velocity vector that contains the gyroscopic and well as Coriolis components and results from differentiating the kinetic energy with respect to

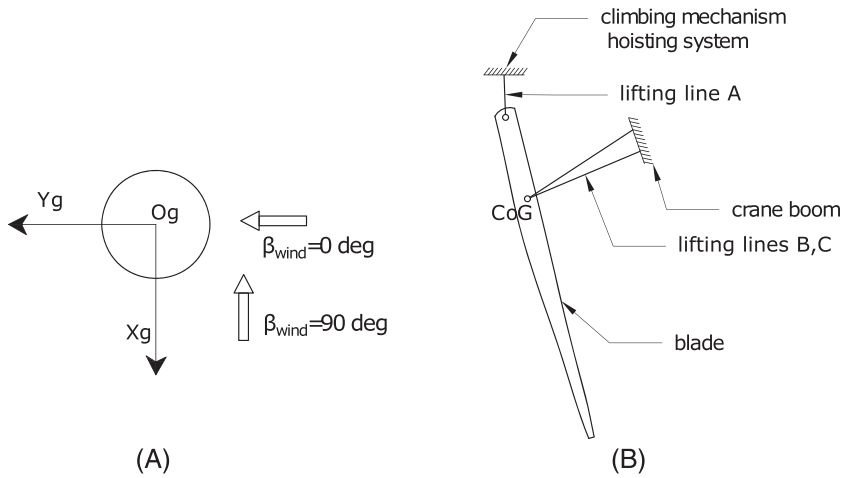

FIGURE 12 Blade structural model and coordinate system. A, Top view of global coordinate system and wind directions; B, simplified blade decommissioning model in HAWC2, comprising the blade, lifting lines, and a gripper or yoke weight located at the COG of the blade

time and with respect to the system generalized coordinates. Details of the multibody formulation and computational algorithms can be found in Shabana.[42]

In structural modeling of HAWC2, the structures are divided into a few independent coupled elements. These elements are connected by joints that allow large translations and rotations. In this work, the structures include the blade, the lifting lines, and a yoke structure, and the system mass and stiffness matrices include these components. Figure 12 illustrates the simplified structural model with the global coordinate system and wind directions. One end of the lifting line (A) is connected to the tower climbing mechanism hoisting system, and the other lifting lines are connected to the crane boom. The externally applied forces, Q_e, correspond to the aerodynamic forces on the blade. The system constraints are the fixed joints at the end of lifting lines and the spherical joints between the lifting line segments. The spherical joints make it possible for the lines to exhibit noncompressible behavior.[10]

The aerodynamic model in HAWC2 uses both deterministic and stochastic wind conditions. The deterministic part of the wind condition includes features such as mean wind velocity, a linear trend, and special shears. The stochastic wind refers to the turbulence model, and in this work, the Mann's turbulence model is applied. Mann's model is based on isotropic turbulence in neutral atmospheric conditions but accounts for nonisotropic turbulence by using the rapid distortion theory.[43] A length scale factor (L_f), an eddy lifetime constant (Γ), and a spectral multiplier ($\alpha\epsilon^{2/3}$) are used to generate a turbulence box, which moves across the hanged blade during the simulation.

For the blade decommissioning scenarios, the blade is hindered from rotating, and the steady aerodynamic lift and drag coefficients are used to determine the wind loads on each blade section. The lift (L) and drag (D) force per length can be calculated from Equations (8) and (9):

$$L = \frac{1}{2}\rho_{air} V_{rel}^2 c C_l, \tag{8}$$

$$D = \frac{1}{2}\rho_{air} V_{rel}^2 c C_d, \tag{9}$$

where ρ_{air} is the air density, V_{rel} is the relative wind velocity seen from the blade, c is the local chord length, and C_l and C_d are the lift and drag coefficients, respectively. According to Gaunaa et al.,[44] computational fluid dynamics methods can be applied to complement this engineering approach.

Time-domain simulations are performed with a time step of 0.01 s. The Newmark-beta method is applied in order to advance the numerical integration and solve for the state vector at each time step. It is assumed that either configuration lasts no more than 10 min. For each case, six 10-min simulations with random wind seeds were carried out to reduce the statistical uncertainties, and the statistical average of the maximum response of each 10-min simulation is used. These number of simulations gave a good representation of response statistics of the system at reasonable computation efforts. [10] Each simulation lasted 1200 s, and the start-up transients 600 s were discarded in the postprocessing.

To investigate the limiting conditions for the blade decommissioning process, a range of wind conditions between 6 and 14 m/s are selected. Two representative wind directions β_{wind} of 0° and 90° for the incoming wind are considered. These directions are chosen because they will produce lift- and drag-dominated conditions, which are of interest to this research. The normal turbulence model (NTM) is considered according to the IEC standard.[45] Based on the NTM, the turbulence standard deviation (STD) for the standard wind turbine class is given by

$$\sigma_1 = I_{ref}(0.75U_{hub} + b), \tag{10}$$

where I_{ref} is the expected value of the turbulence intensity (TI) at 15 m/s, U_{hub} is the hub-height mean wind speed over 10 min, and b is a constant of 5.6 m/s. An I_{ref} of 0.12 is chosen for the wind turbine class C with lower turbulence characteristics in this study. The TI is the ratio of σ_1 and

U_{hub}. Although TI is inversely proportional to U_{hub}, it has a stochastic nature, and a probability distribution of TI was considered in Larsen et al.[46] Here, different combinations of TI and U_{hub} were considered, and TI ranges between 0.06 and 0.26. Moreover, a wind shear exponent of 0.1 that accounts for the vertical wind profile was applied.

4 | RESULTS AND DISCUSSIONS

This section calculates the operational limits for the potentially critical activities and assesses the structural integrity of an OWT tower. In addition, an overall assessment is provided of the feasibility of the proposed OWT blade replacement concept.

4.1 | Analysis of the jack-up vessel

4.1.1 | Dynamic response of the jack-up legs

Dynamic analysis of the jack-up vessel under different wave conditions are performed, and the velocities at the tip of the legs before touching down the seabed are obtained. Figure 13 shows the time series of the velocity components of the Leg1 tip; refer to Figure 10) for two sea states. These two sea states were selected only to compare the influence of wave directions on time histories of dynamic responses. The responses of two wave directions are compared. Because of the roll and pitch resonance motions (refer to the natural periods in Table 3), all the velocity components are higher when T_p is 8 s compared with those when T_p is 6 s. The velocity components in the *Y*-direction (V_y) increase significantly when the wave direction changes from 180° to 135° due to the increase of the vessel roll motions. To further compare the contributions of the different velocity components, Figure 14 presents the STDs of the three velocity components for different T_p conditions. While the *Z*-component (V_z) is less sensitive to wave direction, the *X*- and *Y*-components (V_x and V_y) are influenced greatly by the wave direction. V_x and V_y are induced by the pitch and roll motions of the vessel, respectively, and both motions are sensitive to the wave direction. The most critical condition is observed when T_p is close to 8 s, and the V_y velocity component is dominant when the wave direction is 135°. The velocities of the leg tips determine the allowable sea states for the lowering operation of the jack-up legs.

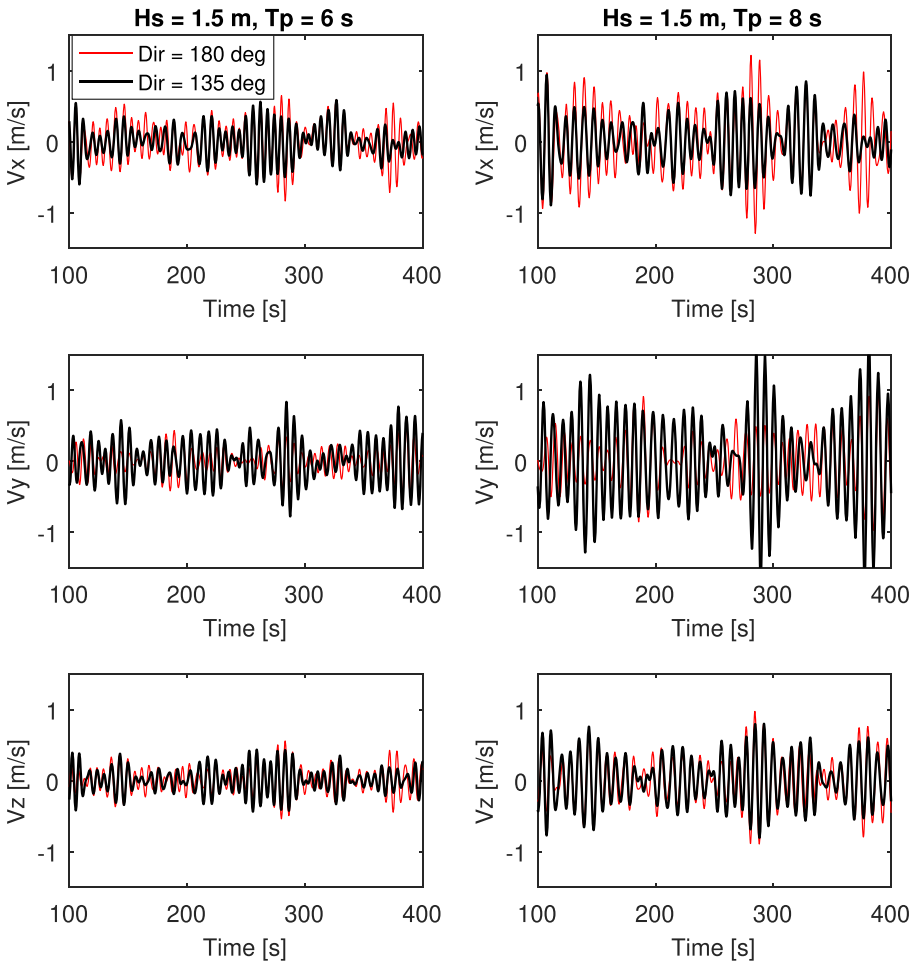

FIGURE 13 Time series of the velocity components of the jack-up leg tip under different conditions [Colour figure can be viewed at wileyonlinelibrary.com]

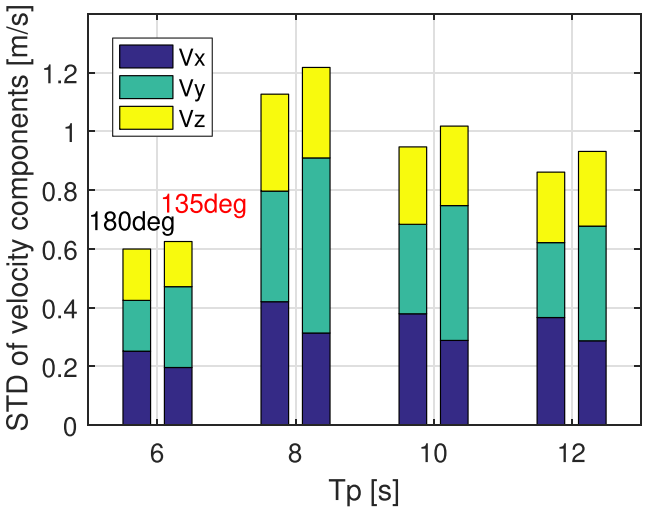

FIGURE 14 Standard deviations of the velocity components of the jack-up leg tip ($H_s = 1.5m$). For each T_p, the left column stands for the wave direction of 180°, and the right column stands for the wave direction of 135° [Colour figure can be viewed at wileyonlinelibrary.com]

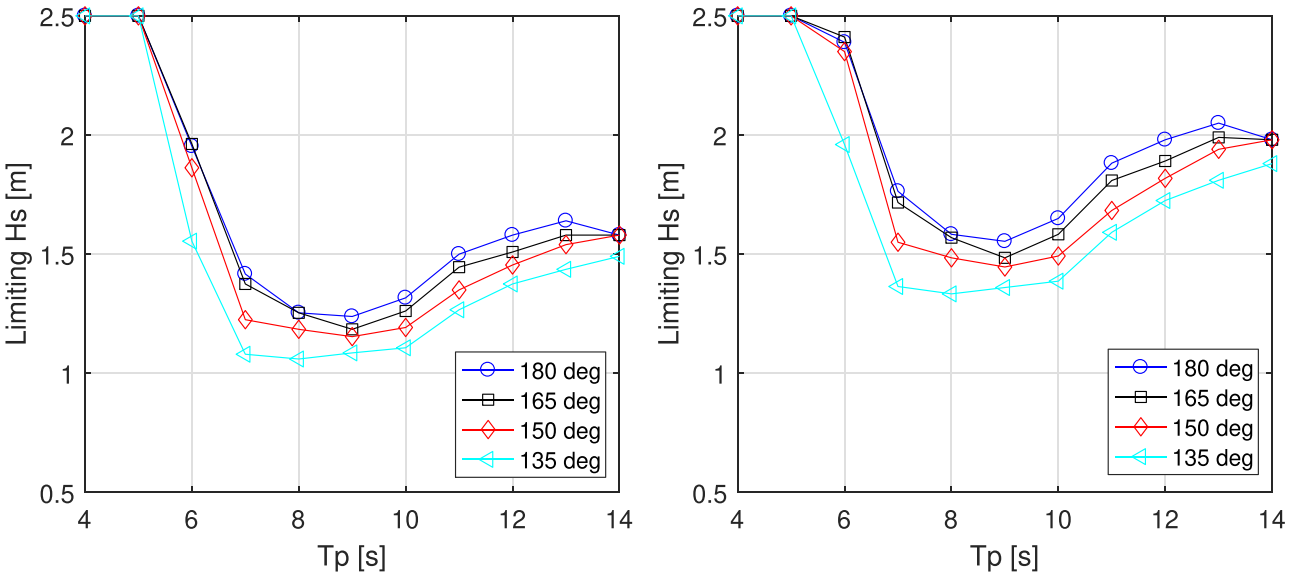

(A) Allowable impact velocity, V_{allow} = 1.6 m/s (B) Allowable impact velocity, V_{allow} = 2.0 m/s

FIGURE 15 Limiting sea states for positioning the jack-up vessel [Colour figure can be viewed at wileyonlinelibrary.com]

4.1.2 | Limiting wave conditions for the jack-up vessel

From the dynamic responses of the jack-up legs under each wave condition, the expected maximum tip velocity of each leg can be obtained. The largest total relative velocity among the four legs is used to find the limiting sea states. The allowable limit of the impact velocity of the leg can be determined by a leg-soil impact analysis.[47] In this case study, this velocity was not derived but reasonably estimated based on information available from Smith et al.[25] For a specific allowable limit of the impact velocity and its corresponding characteristic value, a backward derivation of the corresponding H_s (T_p) limit was performed.[21]

Figure 15 presents the operational limits in terms of allowable sea states for allowable impact velocities of 1.6 and 2.0 m/s, respectively. In the figure, the maximum H_s is limited to 2.5 m. Regardless of the wave direction and load cases, the curves reach a valley near T_p=9 s, which is close to the natural periods of the vessel's roll and pitch. For a fixed wave period, the limiting H_s is lowest at the 135° direction. This is because the vessel experiences more roll motions in quartering seas than in oblique and head seas, and the roll motions are closely related to leg motions. It is possible to further increase the operational limits when waves are coming from the side of the vessel by reducing the roll motions via a passive compensation system.[28]

To position a jack-up vessel at the working site, normally head waves are selected. For the jack-up model selected in this study, Figure 15 shows that the H_s limits vary between 1 and 2.5 m, which are in agreement with an H_s limit of 2.0 m used in industrial practice.[14] Thus, this routine installation activity is feasible because the operational limits are within expected values.

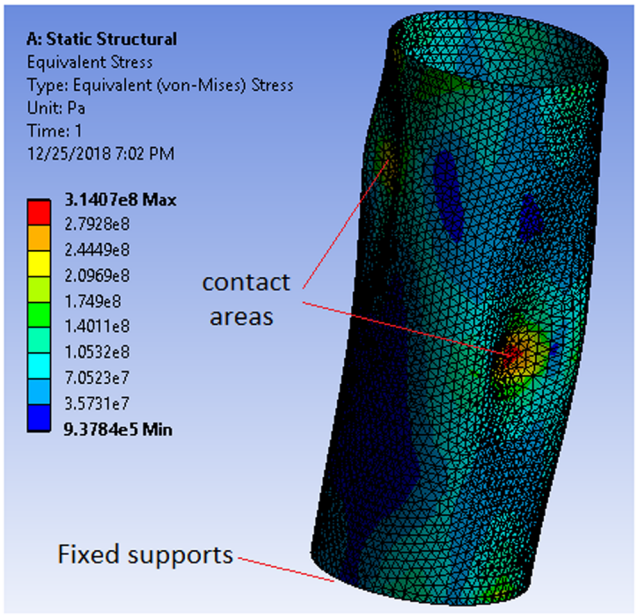

FIGURE 16 Von Mises stresses in the offshore wind turbine (OWT) tower [Colour figure can be viewed at wileyonlinelibrary.com]

4.2 | Structural integrity of the OWT tower

Based on the force analysis conducted in Section 3.2.3, a finite element model of a section of the OWT was established in ANSYS Structural.[48] Figure 16 shows a stress contour of the deformed tower structure after the analysis. The finite element model consists of 24 380 solid elements, and the number of elements are sufficient to achieve convergence. The bottom nodes of the model are fixed, and the external forces exerted by the friction pads of the tower climbing mechanism were applied as pressure loads with a magnitude of 1 MPa, which corresponds to the forces obtained for the configuration shown in Figure 11 and by considering a friction pad with an assumed contact area of 1 m^2. This pressure magnitude will decrease if the contact area is increased. Figure 16 shows that the maximum combined stress is approximately 314 MPa, which is lower than the yield strength of an S355 steel (355 MPa). Such a steel is often used in the construction of OWT towers.[49] Similarly, the maximum deflection of the tower wall is approximately 1.3 mm. Based on these results, it can be concluded that the climbing mechanism will not compromise the structural integrity of the OWT tower.

4.3 | Analysis of the blade system in a lowering process

The two blade configurations shown in Figure 9 are the foci here. First, representative time series of the dynamic responses are shown. Then, the limiting wind conditions derived based on the response maxima are presented.

4.3.1 | Dynamic response of the blade system

During the lowering process, the blade position experiences continuous changes because of the action of the lifting lines and turbulent wind loads. Figures 17 and 18 show the time series of selected responses under the same wind conditions. For Configuration No. 1, at the blade has just been lowered from the hoisting system, the blade orientation is almost vertical, and the lifting line A takes most of the weight of the blade (17.3 tonnes) and yoke (50 tonnes). As illustrated in Figure 17, regardless of the incoming wind direction, the tension in line A is significantly greater than those in the other two lines, and dynamic tension is relatively small compared with the weight. The tensions in lines B and C are at the same level due to the symmetric line configuration. Comparing the two wind directions, we observe that when β_{wind}=0°, the wind speed in the Y_g-component is dominant. Hence, the wind is almost flat to the blade, and the angle of attack fluctuates around 90° in the simulation. This leads to drag-dominated aerodynamic loads, which is preferred during blade installation/decommissioning because of the stability in force directions. In contrast, when β_{wind}=90°, the wind speed is dominant in the X_g-direction, and the angle of attack fluctuates around 0°, leading to a lift-dominated loading situation. In this case, aerodynamic forces will be primarily in the horizontal plane, and the vertical force component and hence the blade response is expected to be small. For this configuration, the blade-root velocity in the Z_g-direction is a primary concern. If this velocity component is too high, the winch may not be able to immediately release the lifting lines and pose risks to the operation. Therefore, the maximum blade-root velocities (red markers) are further used to derive the limiting wind conditions.

The results of Configuration No. 2 are presented in Figure 18. As the blade approaches the end of the lowering process, the blade orientation is more horizontal, and the three lifting lines tend to share the load more evenly. As shown, the mean tension in line A is much reduced compared with that in Configuration No. 1, but the dynamic tension appears to increase, particulary for β_{wind}=90°. The increase in dynamic tension is due to the frequent change in the aerodynamic lift force directions and will lead to large blade responses in the vertical direction. For Configuration

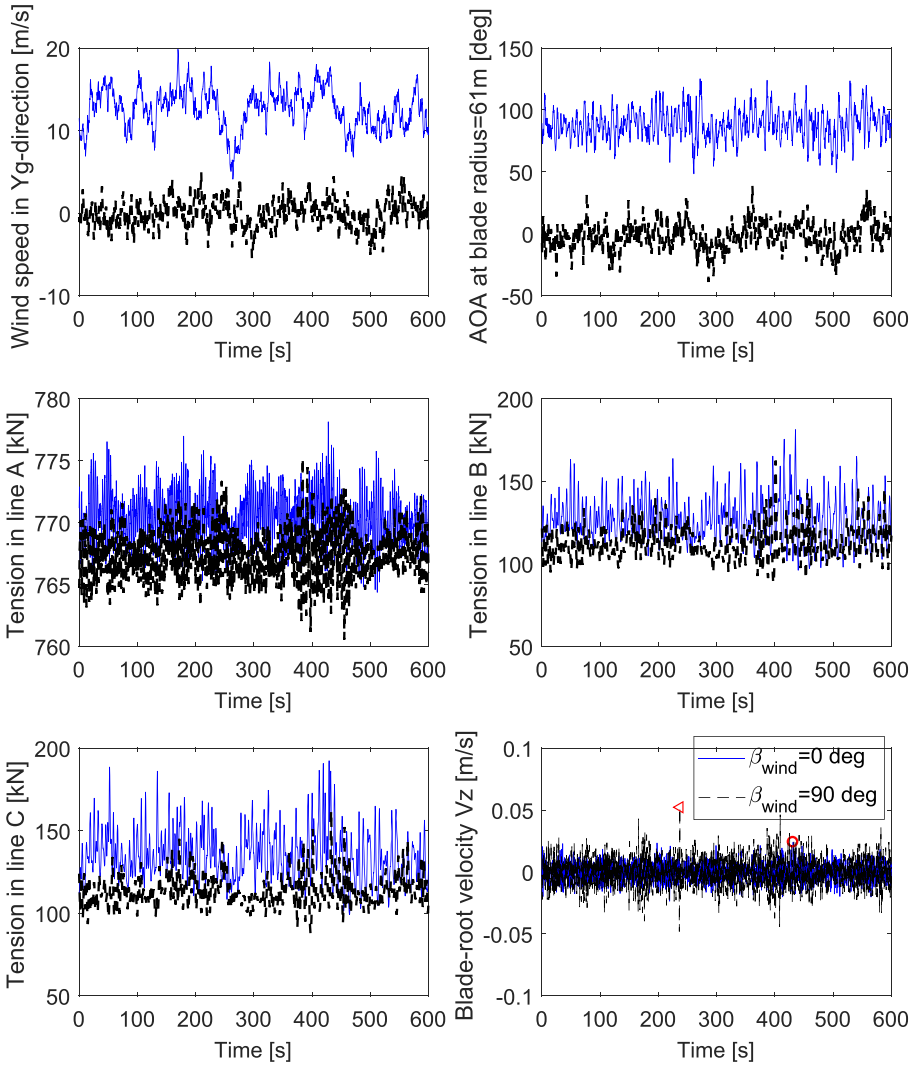

FIGURE 17 Time series of the dynamic responses of Configuration No. 1, U_{hub}= 12 m/s, and TI = 0.2, Seed 1. (AOA denotes angle of attack. The coordinate system is shown in Figure 12) [Colour figure can be viewed at wileyonlinelibrary.com]

No. 2, the mean tension in lifting lines B and C rise considerably, indicating the more important role of the jack-up crane at this moment. For this configuration, the blade-tip velocity in the Z_g-direction is identified as a critical response variable, as a large blade tip velocity poses impact risks. Damages on the blade composite structure during an impact scenario has been previously analyzed.[26] As shown in the time series, the maximum blade-tip velocity V_z becomes much higher when β_{wind} changes from 0° to 90°. This high velocity indicates that the blade decommissioning should be carried out in a milder wind condition.

4.3.2 | Limiting wind conditions

The flexible blade responses are used to derive the limiting wind conditions for the blade lowering operation. Note that the six individual maxima were averaged to derive the limiting conditions. These curves were systematically derived and provide a more comprehensive format to express the operational limits. For Configuration No. 1 shown in Figure 9A, only the blade root velocity is used to limit the operation. Velocity thresholds (allowable impact velocities) of 0.1, 0.2, and 0.3 m/s are used to obtain the limiting wind conditions. Figure 19A shows that for a wind direction corresponding to β_{wind}=0°, the blade-root velocity is always below the threshold levels in all considered turbulence conditions. Thus, the decommissioning of the blade is deemed successful under the largest wind speed of 14 m/s considered in this study. When β_{wind}=90°, large blade motions in the direction of the wind occur. As shown in Figure 19A , the limiting wind speed is 10.26 m/s when the maximum blade velocity of 0.1 m/s and a TI of 0.26 is considered.

Based on the results shown in Figure 19A, it can be judged that the replacement of an OWT blade is practically plausible for all considered wind speeds and turbulence intensity factors when β_{wind}= 0°, because both Configurations No. 1 and 2 shown in Figure 9 are exposed to low risks during turbulent wind conditions. This observation indicates that if the blade orientation relative to the wind direction can be controlled, installation or replacement of an OWT blade is possible.

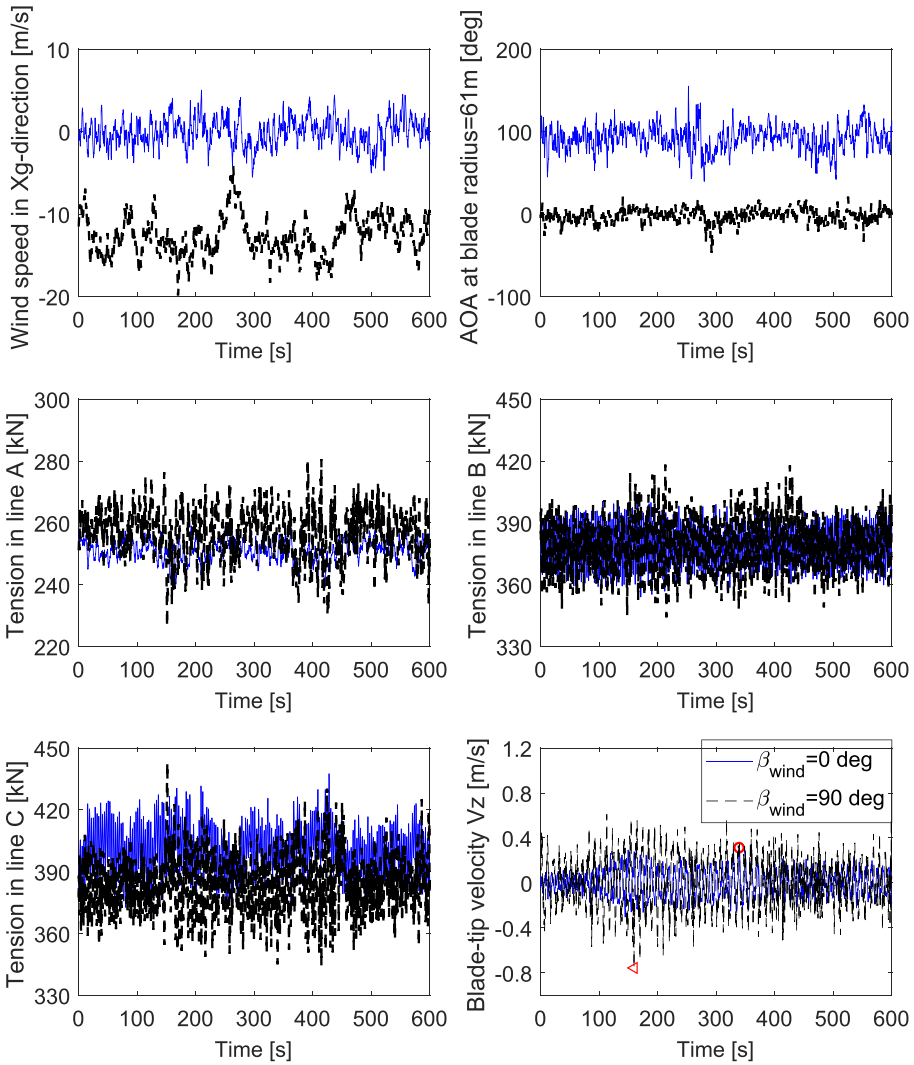

FIGURE 18 Time series of the dynamic responses of Configuration No. 2, U_{hub}= 12 m/s and TI = 0.2, Seed 1. (AOA denotes angle of attack. The coordinate system is shown in Figure 12) [Colour figure can be viewed at wileyonlinelibrary.com]

For Configuration No. 2 shown in Figure 9B, the blade is approaching the deck level. Figure 19B shows that the limiting wind velocities for allowable blade-root velocities of 0.1, 0.2, and 0.3 m/s and β_{wind}=90° are lower than those of Configuration No. 1. This observation is because the blade experiences change in the angle of attack between positive and negative values, leading to increased fluctuations in the direction of the lift forces.

In addition to the blade-root velocity criterion and to avoid possible damage due to impact between the blade and the jack-up vessel, additional threshold limits for the blade-tip velocity should be defined. In this work, allowable blade-tip velocities of 0.2, 0.4 and 0.6 m/s were considered. As it can be observed in Figure 20B, for β_{wind}=90° and especially under high turbulent conditions, for an allowable blade-tip impact velocity of 0.2 m/s, the blade decommissioning is only allowed at low mean wind speeds. Given an allowable impact velocity of 0.2 m/s, and for a TI of 0.15, the limiting wind speed is approximately 10 m/s. Compared with the blade root velocities, the blade tip velocities are larger for the same wind conditions and configuration. The blade tip velocity can be an important parameter that limit the operation because of the risks of impact between the blade tip and the vessel deck.

Despite the fact that a blade root or tip velocity governs the blade lowering operation, Figure 20B shows that even for the worst wind direction, replacement of the OWT blade is feasible. In practice, operations such as mating between a blade and a hub can be performed when the wind speed is up to 12 to 15 m/s.[14] Furthermore, the wind direction information is often available before a lifting operation starts, and β_{wind}=90° can be avoided by the operators. Thus, this operation is feasible because operational limits such as the ones shown in Figure 20A can be obtained.

4.4 | Feasibility assessment

A preliminary assessment of the operational limits for potentially critical installation activities has shown the technical feasibility of this novel installation concept. By applying the current industrial practices, a single 7-MW OWT blade can be installed in 4 to 8 h, and a blade can be replaced between 8 and 16 h.[5] As shown in Table 1, the approximate required installation time is 11 h and similar to the one from the current

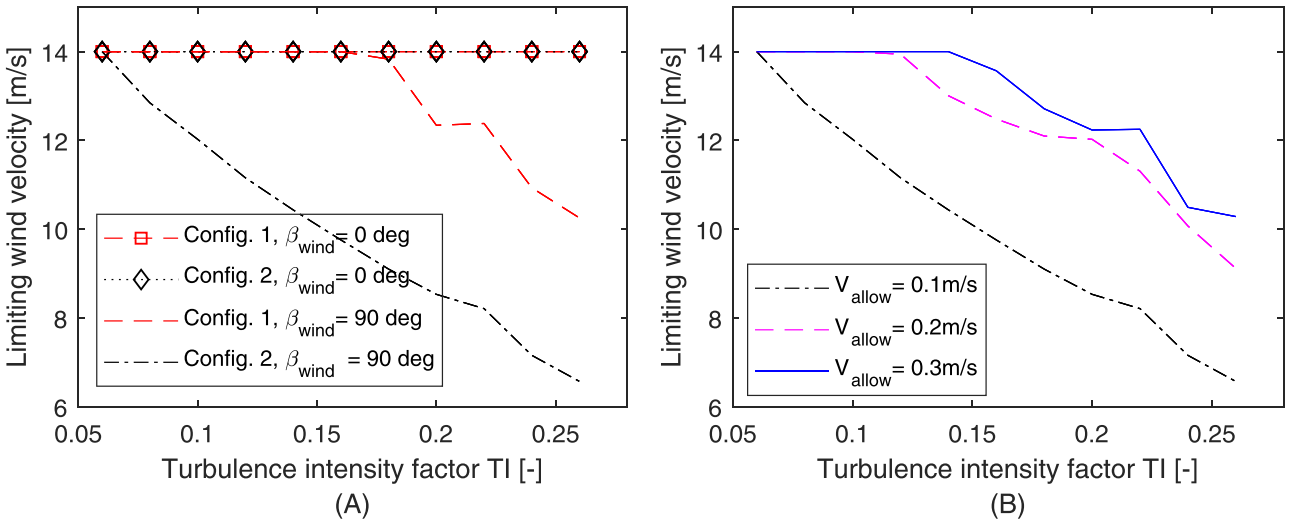

FIGURE 19 Limiting wind velocities for various allowable blade root impact velocities V_{allow}. A, Allowable blade root velocity V_{allow} = 0.1 m/s for β_{wind} = 0° and 90°; B, various allowable blade root velocities for β_{wind} = 90° and Configuration No. 2; refer to Figure 9 [Colour figure can be viewed at wileyonlinelibrary.com]

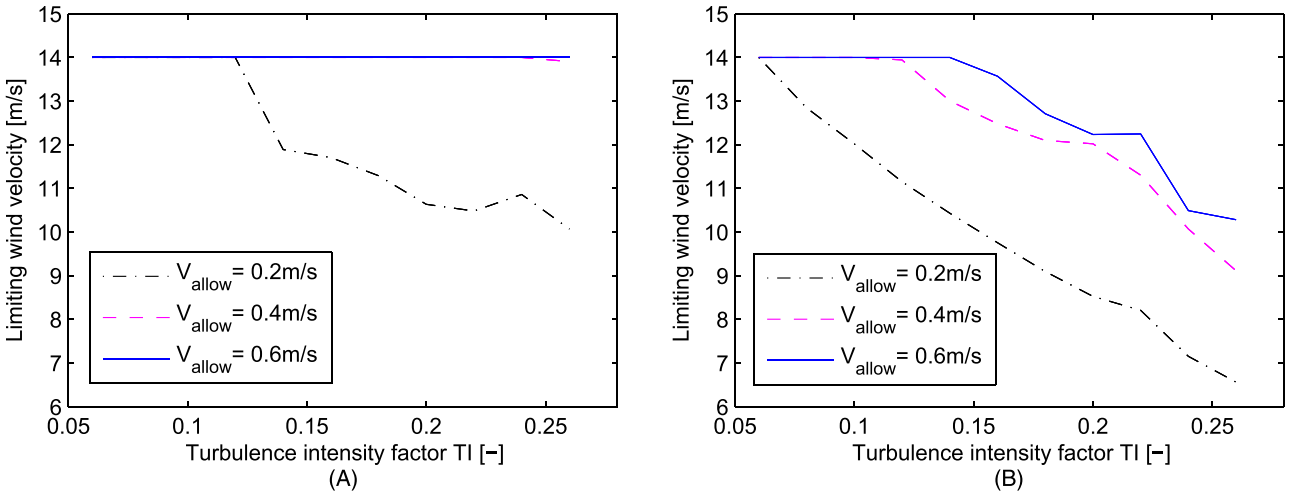

FIGURE 20 Limiting wind velocities corresponding to various allowable blade tip velocities V_{allow} and Configuration No. 2; refer to Figure 9. A, β_{wind} = 0°; B, β_{wind} = 90° [Colour figure can be viewed at wileyonlinelibrary.com]

industrial practices. Because the jack-up lowering and lifting leg operations are similar for the proposed approach and the conventional practices, there is no reduction in the required time for the novel installation concept. However, this concept advocates the use of a small- to medium-sized jack-up crane vessel. Considering the day rate of a medium- to large-sized jack-up barge lies between 100 000 and 180 000 USD,[5,14] the cost reduction of this concept can be significant if a large number of OWTs are to be repaired. A comprehensive cost analysis of the proposed blade installation concept is out of the scope of this work.

5 | CONCLUSIONS AND RECOMMENDATIONS

This paper studies a novel concept for blade installation or replacement of OWTs. The system is composed of a medium-sized jack-up crane vessel and a tower climbing mechanism. The crane vessel is used to install the climbing mechanism and the wind turbine blade, and the mechanism climbs the tower and lowers the blade to the deck of the vessel. Moreover, the same climbing mechanism can be reused for installation or decommissioning of several blades.

Potentially critical installation activities of the novel blade replacement concept are identified. These activities are the positioning of the jack-up vessel, climbing of the mechanism, and lowering of the OWT blade. For these activities, the corresponding response parameters that limit the operations are used to assess the operational limits. These parameters are the impact velocity between the legs of the jack-up vessel and the seabed, the stresses in the wind turbine tower due to contact with the climbing mechanism, and the impact velocities of the blade during the lowering process.

Technical feasibility of the proposed concept is demonstrated through numerical simulations, and operational limits are assessed of the potentially critical marine operation activities. For positioning of the jack-up vessel, the operational limits are established in terms of significant wave height and wave spectral peak period. Based on these results and common industrial practices, the installation activity is shown to be feasible. Regarding the structural integrity of the OWT tower, the stresses caused by the tower climbing mechanism are lower than the yield strength of most structural steels used in tower construction. Finally, for the blade lowering activity, a more comprehensive format for systematically derived limiting curves of the wind speed are provided. These formats for operational limits can be useful to make an on-board decision during execution of marine operations.

Operational limits of installation activities used in the numerical analyses are specifically for the structures considered in this study. In practice, structures can have different dynamic and structural parameters, motion compensation systems can be employed, and blade decommissioning configurations can be optimized. Thus, higher operational limits can be achieved.

To assess the feasibility of the blade lowering activity, steady-state time-domain simulations for two blade configurations are conducted. In future, time-domain simulations of the nonstationary lowering operation are recommended to assess the dynamic responses of the blade and thus to establish the operational limits.

Although several concepts for pole climbing robots exist and the proposed climbing mechanism concept has been tested, multibody simulation of this mechanism including the actual size of structural members and payload should be conducted.

This work assumes a jacket support structure for the OWT and ignores vibrations of the support structure in waves. In future, if monopile foundations are used, global motions of the wind turbine foundation should be considered during modeling of the blade lowering processes and the limiting environmental conditions. The crane boom flexibility can be addressed as well.

Operability analyses of the proposed OWT blade replacement concept can be conducted and compared with those from actual industrial practices.

ACKNOWLEDGEMENTS

The first author acknowledges the support from project PII-DIM-2019-01 "Desarrollo de una metodología para evaluar la factibilidad técnica de operaciones marinas considerando cargas de viento y oleaje marino" granted through the Department of Mechanical Engineering from Escuela Politécnica Nacional.

ORCID

Zhiyu Jiang https://orcid.org/0000-0002-8778-0999

REFERENCES

1. Wu M. Numerical analysis of docking operation between service vessels and offshore wind turbines. *Ocean Eng*. 2014;91:379-388.
2. Spinato F, Tavner PJ, Van Bussel G, Koutoulakos E. Reliability of wind turbine subassemblies. *IET Renew Power Gener*. 2009;3(4):387-401. http://doi.org/10.1049/iet-rpg.2008.0060
3. Renews. Anholt grapples with blade fix. https://renews.biz/110279/anholt-grapples-with-blade-fix/ [Online; accessed 01-October-2018]; 2018.
4. Anderson C. Gearbox replacement needed on turbine 14. http://www.4coffshore.com/windfarms/gearbox-replacement-needed-on-turbine-14-nid6244.html [Online; accessed 26-January-2018]; 2018.
5. Ahn D, Shin S, Kim S, Kharoufi H, Kim H. Comparative evaluation of different offshore wind turbine installation vessels for Korean west–south wind farm. *Int J Naval Archit Ocean Eng*. 2017;9(1):45-54. https://doi.org/10.1016/j.ijnaoe.2016.07.004
6. Guachamin Acero W, Gao Z, Moan T. Numerical study of a novel procedure for installing the tower and rotor nacelle assembly of offshore wind turbines based on the inverted pendulum principle. *J Marine Sci Appli*. 2017;16:243-260. https://doi.org/10.1007/s11804-017-1418-6
7. Guachamin-Acero W, Moan T, Gao Z. Steady state motion analysis of an offshore wind turbine transition piece during installation based on outcrossing of the motion limit state. In: ASME Paper No. OMAE2015-41142, *Proc. of the ASME 34th International Conference on Ocean and Arctic Engineering*; 2015; St. John's, NL, Canada. May 31-June 5, Vol 3 https://doi.org/10.1115/OMAE2015-41142
8. Ren Z, Jiang Z, Skjetne R, Gao Z. Development and application of a simulator for offshore wind turbine blades installation. *Ocean Eng*. 2018;166:380-395. https://doi.org/10.1016/j.oceaneng.2018.05.011
9. Zhao Y, Cheng Z, Sandvik PC, Gao Z, Moan T. An integrated dynamic analysis method for simulating installation of single blades for wind turbines. *Ocean Engineering*. 2018;152:72-88. https://doi.org/10.1016/j.oceaneng.2018.01.046
10. Jiang Z, Gao Z, Ren Z, Li Y, Duan L. A parametric study on the final blade installation process for monopile wind turbines under rough environmental conditions. *Eng Struct*. 2018;172:1042-1056. https://doi.org/10.1016/j.engstruct.2018.04.078
11. Kuijken L. Single blade installation for large wind turbines in extreme wind conditions. *Master of Science Thesis*: Technical University of Denmark & TU Delft; 2015.
12. Jiang Z. The impact of a passive tuned mass damper on offshore single-blade installation. *J Wind Eng Ind Aerodyn*. 2018;176:65-77. https://doi.org/10.1016/j.jweia.2018.03.008
13. Maes K, De Roeck G, Lombaert G. Motion tracking of a wind turbine blade during lifting using rtk-gps/ins. *Eng Struct*. 2018;172:285-292. https://doi.org/10.1016/j.engstruct.2018.06.041
14. Thomsen K. *Offshore Wind: A Comprehensive Guide to Successful Offshore Wind Farm Installation*: Academic Press; 2014.

15. Bense MP. Comparison of numerical simulation and model test for integrated installation of GBS wind turbine. *Master's Thesis*. Trondheim, Norway; 2014.
16. Sarkar A, Gudmestad OT. Study on a new method for installing a monopile and a fully integrated offshore wind turbine structure. *Marine Struct*. 2013;33:160-187. https://doi.org/10.1016/j.marstruc.2013.06.001
17. De Groot K. A novel method for installing offshore wind turbine blades with a floating vessel. *Master's Thesis*; 2015.
18. Lorber Y, Pampalov D. The CLIMBOT, pole climbing robot. www.youtube.com/watch?v=CCHjPtYwhes [Online; accessed 11-January-2018]; 2010.
19. Sadeghi M, Moradi A. Design and fabrication of a column-climber robot (koala robot). *Int J Aerosp Mech Eng*. 2008;2:220-225. https://zenodo.org/record/1330907
20. Jack Up Barge BV. *Specification JB 115*. Labroy Marine Limited, Singapore; 2017. https://www.jackupbarge.com/wp-content/uploads/2017/01/Specification-JB-115-2017.pdf [Online; accessed 05-January-2019].
21. Guachamin Acero Wilson, Li L, Gao Z, Moan T. Methodology for assessment of the operational limits and operability of marine operations. *Ocean Eng*. 2016;125:308-327. https://doi.org/10.1016/j.oceaneng.2016.08.015
22. Guachamin Acero W, Gao Z, Moan T. Methodology for assessment of the allowable sea states during installation of an offshore wind turbine transition piece structure onto a monopile foundation. *J Offshore Mech Arctic Eng*. 2017;139(6):061901. https://doi.org/10.1115/1.4037174
23. Li L, Guachamin Acero W, Gao Z, Moan T. Assessment of allowable sea states during installation of OWT monopiles with shallow penetration in the seabed. *J Offshore Mech Arctic Eng*. 2016;138(4):041902. https://doi.org/10.1115/1.4033562
24. Augener PH, Hatecke H. Sea-keeping analysis of an offshore wind farm installation vessel during the jack-up process. ASME Paper No. OMAE2014-23450 Proc. of the ASME 2014 33rd International Conference on Ocean, Offshore and Arctic Engineering; 2014; San Francisco, USA. June 08-13. doi: V01AT01A031,https://doi.org/10.1115/OMAE2014-23450
25. Smith IAA, Lewis TC, Miller BL, Lai PSK. Limiting motions for jack-ups moving onto location. *Marine Structures*. 1996;9:25-51. https://doi.org/10.1016/0951-8339(95)00002-N
26. Verma AS, Jiang Z, Vedvik NP, Gao Z, Ren Z. Impact assessment of a wind turbine blade root during an offshore mating process. *Eng Struct*. 2019;180:205-222. https://doi.org/10.1016/j.engstruct.2018.11.012
27. Verma AS, Vedvik NP, Haselbach PU, Gao Z, Jiang Z. Comparison of numerical modelling techniques for impact investigation on a wind turbine blade. *Compos Struct*. 2019;209:856-878. https://doi.org/10.1016/j.compstruct.2018.11.001
28. Jiang Z, Guachamin-Acero W, Gao Z, Li L. A numerical study on a flopper stopper for leg positioning of a jack-up barge. In: ASME Paper No. OMAE2017-62034 *Proc. of the ASME 2017 36th International Conference on Ocean, Offshore and Arctic Engineering*; 2017; Trondheim, Norway:V009T12A028. https://doi.org/10.1115/OMAE2017-62034
29. Jonkman J, Butterfield S, Musial W, Scott G. Definition of a 5-MW reference wind turbine for offshore system development. Technical Report No. NREL/TP-500-38060, National Renewable Energy Laboratory, Golden, CO; 2009.
30. SINTEF Ocean. Simo—theory manual version 4.8.4; 2016.
31. Lee C. *Wamit theory manual*: Department of Ocean Engineering, Massachusetts Institute of Technology, USA; 1995.
32. Det Norsk Veritas. Position mooring, offshore standard, DNV-OS-E301; 2013.
33. Ikeda Y, Fujiwara T, Katayama T. Roll damping of a sharp cornered barge and roll control by a new-type stabilizer. In: Proceedings of the 3rd International Society of Offshore and Polar Engineers Conference, Vol. 3; 1993; Singapore:634-639.
34. Det Norsk Veritas. Modelling and analysis of marine operations, DNV-RP-H103; 2011.
35. Hasselmann K, Barnett TP, et al. Measurements of wind-wave growth and swell decay during the joint north sea wave project JONSWAP, Deutches Hydrographisches Institut; 1973.
36. American Society of Civil Engineers. *Minimum Design Loads for Buildings and Other Structures, Standard ASCE/SEI 7-10*: ASCE; 2013.
37. Budynas R, Nisbett JK. *Shigley's Mechanical Engineering Design*: McGraw-Hill Education; 2016.
38. Guachamin Acero W, Gao Z, Moan T. Assessment of the dynamic responses and allowable sea states for a novel offshore wind turbine installation concept based on the inverted pendulum principle. *Energy Procedia*. 2016;94:61-71. https://doi.org/10.1016/j.egypro.2016.09.198
39. Sandvik PC. Estimation of extreme response from operations involving transients. In: 2nd Marine Operations Speciality Symposium MOSS 2012, Singapore; ISBN978-981-07-1896-1; 2012.
40. Larsen TJ, Hansen AM. How 2 HAWC2, the user's manual, Roskilde, Denmark, Risø National Laboratory, Technical University of Denmark; 2012.
41. Kim T, Hansen AM, Branner K. Development of an anisotropic beam finite element for composite wind turbine blades in multibody system. *Renew Energy*. 2013;59:172-183.
42. Shabana A. *Dynamics of Multibody Systems*: Cambridge University Press; 2013.
43. Mann J. The spatial structure of neutral atmospheric surface-layer turbulence. *J Fluid Mech*. 1994;273:141-168. https://doi.org/10.1017/S0022112094001886
44. Gaunaa M, Heinz J, Skrzypiński W. Toward an engineering model for the aerodynamic forces acting on wind turbine blades in quasisteady standstill and blade installation situations. In: Journal of Physics: Conference Series, IOP Publishing, No. 2, Vol. 753; 2016. https://doi.org/10.1088/1742-6596/753/2/022007
45. International Electrotechnical Commission. *Iec 61400-3 wind turbines. part3: Design requirements for offshore wind turbines*. 3rd ed. Geneva, Switzerland: International Electrotechnical Commission; 2009.
46. Larsen GC, Ronold K, Jørgensen HE, Argyriadis K, de Boer J. Ultimate loading of wind turbines, Risø-R-1111(EN), Risø National Laboratory for Sustainable Energy, Technical University of Denmark, Denmark; 1999.
47. Ringsberg JW, Daun V, Olsson F. Analysis of impact loads on a self-elevating unit during jacking operation. In: ASME Paper No. OMAE2015-41030 *Proc. of the ASME 2015 34th International Conference on Ocean, Offshore and Arctic Engineering*; St. John's, Newfoundland, Canada. May 31-June 5.
48. ANSYS, Inc.. Academic research mechanical, release 16.2.

49. Bak C, Zahle F, Bitsche R, et al. Description of the DTU 10 MW reference wind turbine. DTU Wind Energy Report-I-0092, Technical University of Denmark, Fredericia (Denmark); 2013.

How to cite this article: Guachamin-Acero W, Jiang Z, Li L. Numerical study of a concept for major repair and replacement of offshore wind turbine blades. *Wind Energy*. 2020;23:1673-1692. https://doi.org/10.1002/we.2509